Optics Communications 297 (2013) 125–128

Contents lists available at SciVerse ScienceDirect

Optics Communications

journal homepage: www.elsevier.com/locate/optcom

# Dark–antidark solitons in waveguide arrays with alternating positive–negative couplings

Aldo Auditore [a,*], Matteo Conforti [a], Costantino De Angelis [a], Alejandro B. Aceves [b]

[a] CNISM, Dipartimento di Ingegneria dell'Informazione, Università degli Studi di Brescia, Brescia 25123, Italy
[b] Department of Mathematics, Southern Methodist University, Dallas, TX 75275, USA

ARTICLE INFO

*Article history:*
Received 22 November 2012
Received in revised form
29 January 2013
Accepted 30 January 2013
Available online 21 February 2013

*Keywords:*
Guided waves
Binary optics
Kerr effect
Spatial solitons

ABSTRACT

We obtain dark and antidark soliton solutions in binary waveguide arrays with focusing and/or defocusing Kerr nonlinearity and with alternating positive and negative linear couplings between adjacent waveguides. For both stationary and moving solitons, we analyze the properties of these solutions in the presence of uniform and nonuniform nonlinearity along the array.



## 1. Introduction

In the last years, discrete optical systems and waveguide arrays have been a very active research area in optics [1]. Binary waveguide arrays in particular have been studied because their intrinsic two bands structure can be very helpful in order to control wave propagation in the linear and nonlinear regimes [2–4]. More recently, the interplay between plasmonic waveguiding and periodicity has been also considered, inasmuch as plasmonic confinement offers an extra degree of freedom to be usefully exploited in all optical devices [5–8].

In this framework solitons represent an important class of solutions, as their particle like behavior can be very useful for switching applications and their peculiar features often represent an invaluable tool to understand the overall dynamics of the system in the nonlinear regime. This certainly explains the huge effort that the scientific community has put in finding soliton solutions in these systems [4,9–14].

It is well known that in nonlinear discrete systems as those describing light propagation in waveguide arrays, bright localized modes may exist in the form of gap solitons when a gap opens in the linear dispersion relation [13,15]. On the other hand, without the band gap in the linear dispersion relation, a forbidden frequency region can still exist for a nonuniform nonlinear response and solitons sitting on a pedestal can be found [14,16,17]. Among the situations where the nonuniform nonlinearity can be exploited it is certainly worth quoting the case of the linear–nonlinear interlaced waveguide arrays [18].

In previous papers we have used a continuous approximation to exploit bright solitary wave solutions of this system [13] and we have then used a fully discrete model to explore the existence and stability of solitons sitting on a nonzero background [14]. In this paper we extend the continuous approximation to the case of a nonzero background and we demonstrate that this continuous approximation can capture many features of the discrete system; remarkably we also show that the continuum approximation gives a reasonable description of discrete states even when they are confined to a very small number of sites.

## 2. Physical settings and theoretical analysis

According to the coupled mode theory and taking into account third-order nonlinearities in the form of a pure Kerr effect, the field amplitude propagation in a binary waveguide array can be described by the following equations [10,13]:

$$iE'_{nz}+\beta_n E'_n+C_{n-1}E'_{n-1}+C_{n+1}E'_{n+1}+\chi_n|E'_n|^2E'_n=0$$

where $E'_n$ is the amplitude of the modal field of the $n$-th waveguide, $\beta_n$ is the propagation constant of each waveguide, $\chi_n$ is the site-dependent nonlinear coefficient, and $C_{n\pm1}$ is the coupling coefficient of the $n$-th waveguide with the $(n\pm1)$-th waveguides. In our case $C_{n-1}=C_1$ and $C_{n+1}=C_2$ when $n$ is even, whereas $C_{n-1}=C_2$ and $C_{n+1}=C_1$ when $n$ is odd. Then, performing the transformation $E'_n=E_n\exp(i\beta z)$, we can separately consider the mode amplitudes in the even and odd waveguides. In this way the field amplitude propagation can be described by the following

* Corresponding author. Tel.: +390 340 286 0431.
*E-mail address:* aldo.auditore@ing.unibs.it (A. Auditore).

0030-4018/$ - see front matter © 2013 Elsevier B.V. All rights reserved.
http://dx.doi.org/10.1016/j.optcom.2013.01.068

two sets of coupled equations with constant coefficients:

$$iA_{nz}+\frac{\Delta\beta}{2}A_n+C_1B_n+C_2B_{n+1}+\gamma_1|A_n|^2A_n=0$$
$$iB_{nz}-\frac{\Delta\beta}{2}B_n+C_2A_{n-1}+C_1A_n+\gamma_2|B_n|^2B_n=0 \quad (1)$$

where $A_n$ and $B_n$ are respectively the mode amplitudes in the $n$-th even and $n$-th odd waveguides, $\chi_n$ was defined $\gamma_1$ ($\gamma_2$) for $n$ even (odd), and we chose $\beta_n=\beta+\Delta\beta/2$ for $n$ even, and $\beta_n=\beta n-\Delta\beta/2$ for $n$ odd, so $\Delta\beta$ represents the difference between the propagation constants in even and odd waveguides. Finally, without loss of generality we can set $C_2=1$ (see [19]).

In close proximity of the band edge (i.e. around $k_x=0$ for $C_1<0$ and for $k_x$ around $\pi$ for $C_1>0$) a very useful equivalent continuous model can be derived by performing a Taylor expansion to obtain (as a first order approximation)

$$iu_z+\frac{\Delta\beta}{2}u+w_x+\epsilon w+\gamma_1|u|^2u=0$$
$$iw_z-\frac{\Delta\beta}{2}w-u_x+\epsilon u+\gamma_2|w|^2w=0 \quad (2)$$

where we have also defined $C_1=\pm1+\epsilon$, with the $-(+)$ sign that has to be used for $k_x=0$ ($k_x=\pi$). To look for both stationary and walking self confined solutions of the system defined by Eq. (2), we use the following trial functions [20]:

$$u(x,z)=\tfrac{1}{2}(K_1g_1(\xi)+iK_2g_2(\xi))\exp(i\cos(Q)\psi)$$
$$w(x,z)=\frac{1}{2i}(K_1g_1(\xi)-iK_2g_2(\xi))\exp(i\cos(Q)\psi)$$
$$\xi=\frac{x+vz}{\sqrt{1-v^2}},\quad \psi=\frac{vx+z}{\sqrt{1-v^2}}$$
$$K_1=\left(\frac{1+v}{1-v}\right)^{1/4},\quad K_2=\left(\frac{1-v}{1+v}\right)^{1/4} \quad (3)$$

with $g_{1,2}$ two arbitrary complex functions, $-1<v<1$. Although not necessary, for the sake of clarity, from now on we set $\Delta\beta=0$.

Substituting the ansatz (3) into Eq. (2) and following the procedure as in [13], it is straightforward to obtain an Hamiltonian form for the equations, observing that $P=|g_1|^2-|g_2|^2$ is a constant of motion for the dynamical system. Indeed, setting $g_{1,2}(\xi)=f_{1,2}(\xi)\exp[i\theta_{1,2}(\xi)]$, $\eta=f_2^2$ and $\mu=\theta_1-\theta_2$, $\eta$ and $\mu$ obey the following Hamiltonian system:

$$\dot\eta=-\frac{\partial H}{\partial\mu}$$
$$\dot\mu=\frac{\partial H}{\partial\eta}$$
$$H=2\eta\cos Q+2\sqrt{\eta(\eta+P)}\epsilon\cos\mu$$
$$-\frac{s}{8}\eta\left[\eta\left(\frac{K_1^4}{2}+\frac{K_2^4}{2}+2-\cos(2\mu)\right)+P(K_1^4+2-\cos(2\mu))\right]$$
$$-\frac{d}{4}\sqrt{\eta(\eta+P)}(\eta(K_1^2+K_2^2)+PK_1^2)\sin\mu \quad (4)$$

where we also set $s=\gamma_1+\gamma_2$ and $d=\gamma_1-\gamma_2$.

It is straightforward to show that this Hamiltonian has the following symmetry: mapping $P$ and $v$ into $-P$ and $-v$ induces only a non nonessential shift by a constant into the Hamiltonian's value. For this reason, from now on we set $P\geq0$. Note also that the Hamiltonian system described by Eq. (4) reduces obviously to the one considered in [13] for $P=0$. Moreover in the situation considered in [13] the condition $\epsilon\neq0$ was necessary in the quest for bright soliton solutions; here, on the contrary, we are interested in discussing solitons with a nonzero background and their existence is not related to the presence of a band gap in the linear spectrum, i.e. they exist even in the case $\epsilon=0$ as we have discussed in [14]. As a matter of fact, the key properties of these solutions sitting on a nonzero background do not depend on the presence of a bandgap in the linear spectrum; for these reasons from now on we consider the case $\epsilon=0$, corresponding to the presence of a Dirac point at zero transverse momentum in the linear spectrum. Soliton solutions of Eq. (2) correspond to separatrix trajectories emanating from and sinking into unstable fixed points of the dynamical system described by Eq. (4).

Obviously the validity of the continuum approximation becomes more questionable as the degree of localization of the solitons increases; in order to get a feeling of how far one can push the use of the continuum model while still having a reasonable description of the discrete system, we performed a thorough comparison between the approximated soliton solutions obtained in the continuum limit and exact soliton states obtained numerically using the Newton conjugate-gradient method [21].

To summarize our findings we report in Fig. 1 the comparison between the modulus of the approximated soliton states obtained from the continuum limit (blue crosses and dashed line) and exact numerical results obtained using the Newton conjugate-gradient method (red open circles). Note that despite the very strong degree of localization (the soliton structure is basically confined to five sites only), the continuum approximation still shows an excellent agreement with the exact solution and this holds true both for the modulus (reported in Fig. 1) and the phase (not shown here). It is worth highlight that in the transition from discrete system to the continuum limit we lost some features. In fact, if we further increase the degree of confinement, we gradually loose the validity of the continuum approximation and for soliton states confined to three sites only the continuum approximation is not able to capture closely the features of the discrete solutions. For such an high level of

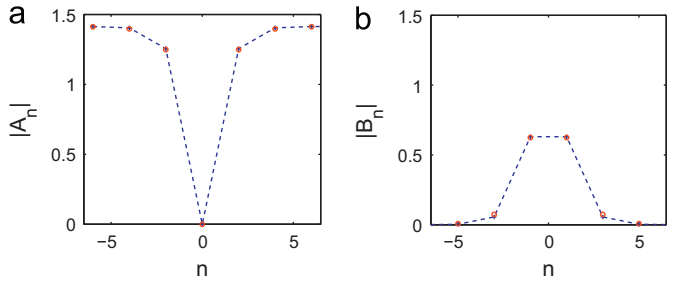


**Fig. 1.** Comparison between approximated soliton states obtained from the continuum limit (blue crosses and dashed line) and exact numerical results obtained using the Newton conjugate-gradient method (red open circles). With reference to Eq. (1) here we set $\gamma_1=1$, $\gamma_2=0$, $C_1=-1$, $C_2=1$, $\Delta\beta=0$ and $\lim_{n\to\pm\infty}|A_n|=\sqrt{2}$. (a) Even sites. (b) Odd sites. (For interpretation of the references to color in this figure caption, the reader is referred to the web version of this article.)

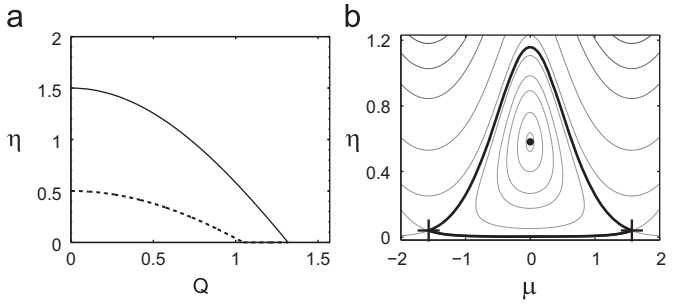


**Fig. 2.** $s=2$, $d=0$, $P=1$, $v=0$. (a) Bifurcation diagram of the Hamiltonian system: continuous lines for stable centers and dashed lines for unstable saddle points. (b) Phase plane analysis ($Q=1$): crosses correspond to the unstable points and the dot shows the stable center. The thicker lines are the heteroclinic separatrices connecting the two unstable saddles and correspond to solitons on a nonzero background.

confinement one has to go back to the discrete model and find their solutions as was recently done by using asymptotic expansions in [14]. It is remarkable to note that by using these two different approximations (asymptotic expansion and continuum model) one can describe in a simple and accurate fashion the entire spectrum of the dark–antidark soliton states of this system.

The derived Hamiltonian system thus represents a valuable tool in describing and in understanding the features of the solutions of the problem; the goal of the rest of the paper is to prove that thanks to this hamiltonian system we are able to introduce new soliton solutions for the problem at hand. Solutions obtained from our continuum model will be used as initial conditions to the discrete model to test their validity and robustness. The above goals will be pursued in next sections using some representative examples; we thus focus our attention on three different binary arrays: the first case we discuss is the case of uniform nonlinearity in the array; the second case we face is that of the linear–nonlinear interlaced binary array and the third one is the case of nonlinearities with different signs along the array, i.e. the focusing–defocusing interlaced binary waveguide array.

## 3. Examples

In this section we present some results derived from the analysis of the Hamiltonian system (Eq. (4)). We thus first look for unstable fixed points of the dynamical system and then obtain the separatrices corresponding to solitary wave solutions. To assess the validity of our approach we then propagate the obtained waveforms in the truly discrete system described by Eq. (1). If we were looking for bright solitons, as we did in [13], we would pick $P=0$ and this in turn would simplify considerably the algebra required in the analysis of the dynamical system described by Eq. (4); here, instead, we focus on the general case $P\neq 0$. As a first example, we consider an array with uniform nonlinearity (i.e. $d=0$). In Fig. 2a we report the bifurcation diagram of the amplitude $\eta$ of the fixed points as a function of $Q$; unstable fixed points and thus dark solitons do exist only for $Q<\arccos(sP(3+k_1^2)/16)$; note that the unstable fixed points here correspond to two different branches with different generalized phase ($\mu=\pm\pi/2$). In Fig. 2b we report the phase plane analysis of the system and we see two saddle points at $\mu=\pm\pi/2$ and $\eta=(16\cos(Q)-sP(K_1^4+3))/(s(K_1^4+K_2^4+6))$; the separatrices emanating from and sinking into the saddles turn around the center located at $\mu=0$ and $\eta=(16\cos Q-sP(K_1^4+1))/(s(K_1^4+K_2^4+2))$. The existence of these saddle points is possible if the following constraints on $Q$ and $P$ are satisfied: $0<Q<\arccos(sP(K_1^4+3)/16)$ and $0<P<16/(s(K_1^4+3))$.

To test the validity of these results we use the obtained solutions as the initial condition (i.e. at $z=0$) in the numerical integration of the equations describing propagation in the binary waveguide array (i.e. Eq. (1)); the results are reported in Fig. 3a where the initial condition corresponds to the trajectory enlightened with a thicker line in the inset of the figure.

Note that propagation of this solution into the array reveals only a small amount of radiation (almost nonvisible) thus proving the validity of the continuum approximation. Moreover, these solutions are strong enough to survive for nonzero transverse velocities: in Fig. 3b we report one example of nonzero transverse velocity and we observe once again that the continuum system is able to capture the nature of the discrete one. Also in this case the amount of emitted radiation is negligible.

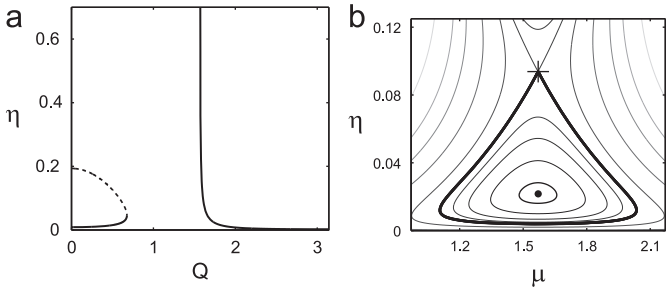


**Fig. 4.** $s=2$, $d=2$, $P=0.6$, $v=0$. (a) Bifurcation diagram of the Hamiltonian system: continuous lines for stable centers and dashed lines for unstable saddle points. (b) Phase plane analysis ($Q=0.6$): the cross corresponds to the unstable point and the dot shows the stable center. The thicker line is the homoclinic separatrix corresponding to solitons on a nonzero background.

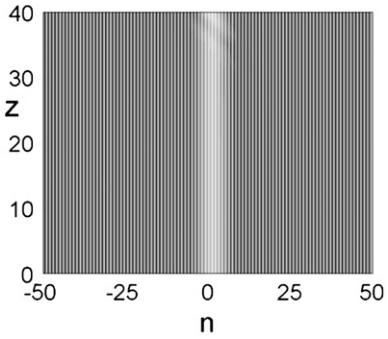


**Fig. 5.** Field evolution along the array: the initial condition corresponds to the separatrix enlightened in Fig. 4b.

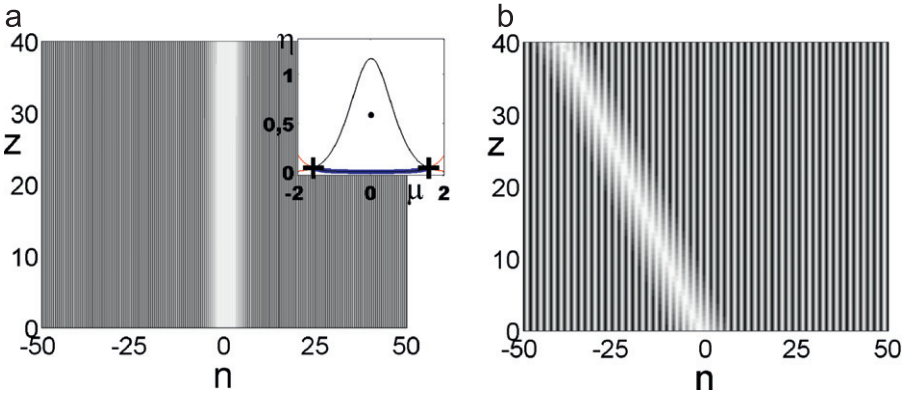


**Fig. 3.** Field evolution along the array for $s=2$, $d=0$, $P=1$: the initial condition is the dark soliton solution corresponding to the thicker line in the inset where the phase plane of system 4 is reported. (a) $Q=1$ and $v=0$. (b) $Q=0.7$ and $v=0.5$.

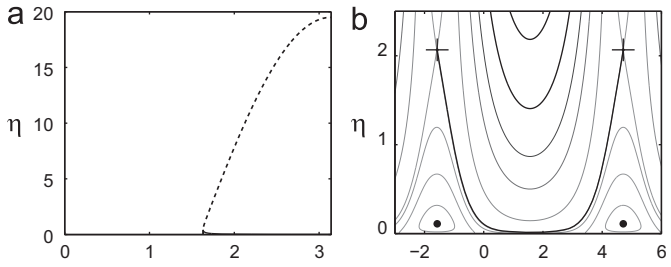


**Fig. 6.** $s=2$, $d=2.1$, $P=1.0$, $\nu=0$. (a) Bifurcation diagram of the Hamiltonian system: continuous lines for stable centers and dashed lines for unstable saddle points. (b) Phase plane analysis ($Q=1.7$): the crosses correspond to the unstable points and the dots show the stable centers. The thicker line is the heteroclinic separatrix corresponding to solitons on a nonzero background.

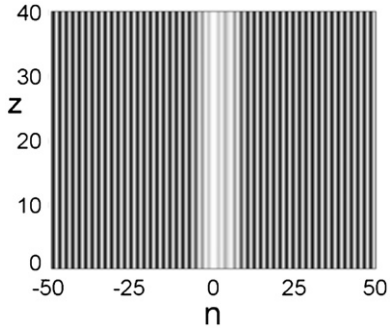


**Fig. 7.** Field evolution along the array for $s=2$, $d=2.1$, $Q=1.7$, $P=1$ and $\nu=0$. The initial condition corresponds to the separatrix enlightened in Fig. 6b.

As a second example we consider the case of an array of alternating linear–nonlinear waveguides, i.e. $s=d$. The situation is quite different with respect to the $d=0$ case: two fixed points (one center and one saddle) exist for $Q<\pi/2$ whereas only one stable center exists for $Q>\pi/2$ (see Fig. 4a). In Fig. 5 we report the beam propagation along the array using as initial condition the field profiles obtained from Eq. (3) after having solved for the trajectory along the separatrix described as a thick line in Fig. 4b. The third example we consider corresponds to an array of alternating focusing–defocusing nonlinearities, i.e. $d>s$ ($s=2$ and $d=2.1$ in what follows). As we can see in Fig. 6a, for $Q>\pi/2$ we find one center and one saddle. In the corresponding phase plane in Fig. 6b we report the heteroclinic trajectory emanating from and sinking into the saddle points at $\mu=-\pi/2$ and $\mu=2\pi-\pi/2$. In Fig. 7 we show the field evolution along the array using as initial condition the field profiles obtained from Eq. (3) and corresponding to the separatrix enlightened in Fig. 6b. Once again we can observe that propagation of this solution into the array reveals again a negligible amount of radiation thus proving the validity of our analytical approach.

## 4. Conclusions

In this work we have obtained dark and antidark soliton solutions in a binary waveguide array with alternating positive and negative linear couplings between adjacent waveguides and in the presence of focusing and/or defocusing Kerr nonlinearity. These solutions do exist also in a linear–nonlinear interlaced array and they even survive in focusing–defocusing interlaced arrays. We have also numerically verified the soundness of our approach by a detailed comparison with exact results obtained by numerically solving the discrete system; remarkably our results, obtained in the framework of a continuum approximation, retain their validity also for very strong degrees of localization.

## Acknowledgments

The authors wish to thank Professor T.R. Akylas for very helpful discussions. A.A., C.D.A. and M.C. acknowledge financial support from CARIPLO Foundation under Grant no. 2010-0595 and US ARMY under Grant no. W911NF-12-1-0202.

## References

[1] F. Lederer, G.I. Stegeman, D.N. Christodoulides, G. Assanto, M. Segev, Y. Silberberg, Physics Reports 463 (2008) 1.
[2] S. Longhi, Optics Letters 31 (2006) 1857.
[3] M. Guasoni, A. Locatelli, C. De Angelis, Journal of the Optical Society of America B 25 (2008) 1515.
[4] N.K. Efremidis, P. Zhang, Z. Chen, D.N. Christodoulides, C.E. Rüter, Detlef Kip, Physical Review A 81 (2010) 053817.
[5] M. Conforti, M. Guasoni, C. De Angelis, Optics Letters 33 (2008) 2662.
[6] M. Guasoni, M. Conforti, C. De Angelis, Optics Communications 283 (2010) 1161.
[7] S.H. Nam, E. Ulin-Avila, G. Bartal, X. Zhang, Optics Letters 35 (2010) 1847.
[8] C.M. de Sterke, L.C. Botten, A.A. Asatryan, T.P. White, R.C. McPhedran, Optics Letters 29 (2004) 1384.
[9] Y.S. Kivshar, A.A. Sukhorukov, Optical Solitons: From Fibers to Photonic Crystals, Academic Press, San Diego, 2003.
[10] A.A. Sukhorukov, Y.S. Kivshar, Optics Letters 27 (2002) 2112.
[11] R. Morandotti, D. Mandelik, Y. Silberberg, J.S. Aitchison, M. Sorel, D.N. Christodoulides, A.A. Sukhorukov, Y.S. Kivshar, Optics Letters 29 (2004) 2890.
[12] A.A. Sukhorukov, Y.S. Kivshar, Optics Letters 30 (2005) 1849.
[13] M. Conforti, C. De Angelis, T.R. Akylas, Physical Review A 83 (2011) 043822.
[14] M. Conforti, C. De Angelis, T.R. Akylas, A.B. Aceves, Physical Review A 85 (2012) 063836(1–4).
[15] A. Marini, A.V. Gorbach, D.V. Skryabin, Optics Letters 35 (2010) 3532.
[16] Y.S. Kivshar, Physical Review Letters 70 (1993) 3055.
[17] N. Flytzanis, B.A. Malomed, Physics Letters A 227 (1997) 335.
[18] K. Hizanidis, Y. Kominis, N.K. Efremidis, Optics Express 22 (2008) 18296.
[19] E.W. Laedeke, K.H. Spatschek, S.K. Turitsyn, Physical Review Letters 73 (1994) 1055.
[20] A.B. Aceves, S. Wabnitz, Physics Letters A 141 (1989) 37.
[21] J. Yang, Journal of Computational Physics 228 (2009) 7007.